Understanding the Discharge Characteristics of Lithium Iron Phosphate and Lithium Cobalt Oxide Cathode Materials

M.S.A. Muhamad Saripudin[1], R. Ranom[2*], I.W. Jamaludin[2], U. Habibah[3]
[1]Cohu Malaysia, No. 5203- 1, Fasa 4, Malaysia, Jalan Pak 2/3, Kawasan Perindustrian Ayer Keroh, 75450 Ayer Keroh, Melaka,Malaysia
[2]Faculty of Electrical Engineering, Universiti Teknikal Malaysia Melaka, Hang Tuah Jaya, 76100 Durian Tunggal, Melaka, Malaysia
[3]Mathematics Department, Brawijaya University, Jl. Veteran Malang, East Java, Indonesia.

[*]corresponding author's email: rahifa@utem.edu.my

Abstract – *This paper focuses on the discharge characteristics of two cathode materials, namely Lithium Iron Phosphate ($LiFePO_4$) and Lithium Cobalt Oxide ($LiCoO_2$). The two cathode materials have different discharge characteristics and maximum concentrations. A mathematical model of lithium ion battery (LIB) for half-cell cathode based on drift-diffusion model is used to model the practical operations of LIB. This model takes into account the electrolyte equation and lithium transport equation in the electrode particles and is solved numerically using the Method of Line technique. The simulated discharge curves for both cathode materials have been verified with experimental data. The results show that $LiCoO_2$ has an advantage of high maximum concentration, but the discharge drops with changes in the amount of lithium inserted. Meanwhile, $LiFePO_4$ has the characteristic of a flat discharge curve which gives almost the same power with changes of the inserted lithium until the cell is entirely discharged. The main factor that limits the discharge as the discharge current increases is the Lithium ion depletion region and the saturated of Lithium in the electrode.*

Keywords: *Discharge characteristics, Lithium Cobalt Oxide, Lithium ion battery, Lithium Iron Phosphate*

Article History
Received 2 February 2024
Received in revised form 17 September 2024
Accepted 17 September 2024

I. Introduction

Lithium-ion batteries are being used in various applications such as portable electronics, electric vehicles, and renewable energy systems. The development of lithium-ion batteries has become a key focus for researchers and automotive companies, as the markets for hybrid electric vehicles, plug-in hybrid vehicles, and purely electric vehicles are expected to grow substantially. [1] – [2].

Lithium-ion is made of several elements; the electrodes which are the cathode and the anode, the electrolyte, the separator, and the current collector as shown in Fig. 1. The function of the electrolyte is to allow the ions to travel forth and back from anode to cathode. There are two different polarity types of electrodes which are cathode that are positively charged and is frequently referred to as the working electrode, and another one is anode, which is negatively charged and is frequently referred to as the counter electrode.

The cathode, which is the primary determinant of cell attributes, is typically built of different chemistries than the anode, which is typically formed of silicon or graphite. Examples of cathode materials are Lithium Cobalt Oxide, Lithium Manganese Oxide, and Lithium Iron Phosphate. Each material of cathode has its characteristics hence providing different discharge capabilities.

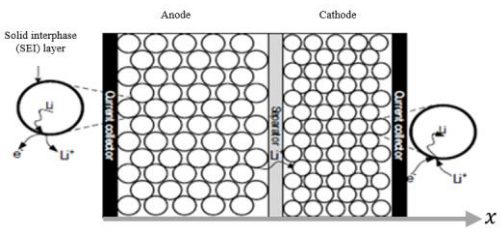

Fig. 1 Schematic of the Lithium-ion cell structure [1]

Lithium iron phosphate ($LiFePO_4$) as a positive electrode material has numerous advantages for lithium ion batteries. $LiFePO_4$ materials can enhance the high-temperature cycle performance of lithium ion batteries, thereby resulting in reduced cost, minimal internal resistance, commendable safety standards, rapid charging speed, and enhanced design capacity [3] – [4]. Lithium cobalt oxide ($LiCoO_2$) cathode offers high volumetric energy density and favorable durability, making it a promising material for lithium-ion batteries [5]. The advantages of using $LiCoO_2$ include high capacity, high-rate properties, and good structural stability.

The rate limitation in $LiFePO_4$ electrodes, initially, was attributed to poor conductivity, but carbon coating has improved electronic conduction. This can be done by using carbon black as a binder and leaving open porosity for the electrolyte [3]. Carbon coating also significantly improves the performance of $LiFePO_4$ in a nano-structured electrode. Hence, Lithium diffusion is not a discharge limiting factor for nanoscale electrode particles. However, high discharge rates of $LiFePO_4$ are restricted by electrolyte diffusion and depletion [4].

The factor limiting discharge in $LiCoO_2$ batteries is poor cycle performance [6] due to the structural instability and severe capacity fade when cycled to voltages greater than 4.35V [7]. Additionally, the asymmetry in discharge/charge behavior toward high bulk stoichiometry (low state of charge) is also a limiting factor [8]. The two-step reaction mechanism involving lithium-ion adsorption onto the active material particle surface and intercalation of surface-adsorbed lithium atoms into the bulk material can reproduce this behavior [9] – [10]. Another factor limiting the discharge is the large volumetric variation of cobalt sulfide during charge/discharge cycling [11]. Different cathode materials have different energy densities, cost implications, and safety profiles. Hence, understanding cathode materials is crucial in improving the cell performance.

This paper discusses the solutions of half-cell cathode of two cathode materials, namely Lithium Cobalt Oxide ($LiCoO_2$) and Lithium Iron Phosphate ($LiFePO_4$) by generating the discharge curves to analyze the battery performance. A comparison study of the discharge characteristics between the two lithium-ion cathode materials is discussed.

II. Lithium-ion Battery mechanism and its mathematical model

A. Electrochemical Mechanism of Lithium-ion Batteries

The electrochemical events are caused by the electrostatic potential difference between the electrodes during discharge. In the active-phase negative electrode's spherical-like particles, the lithium diffuses from the bulk to the surface, where a de-intercalation process takes place. Passing the separator, the lithium, now in the form of ions in the electrolyte phase, goes from the negative electrode to the positive electrode. Due to the separator's electrical insulation, the electrons emitted in the negative electrode following the reaction are simultaneously driven out of the battery. The positive electrode is where the electrons return to the battery after accomplishing electrical work [12]. The lithium-ion undergoes a similar reaction when it comes to the surface of a positive electrode (cathode), where it intercalates into the electrode particle and absorbs an electron from the electrode in the process. On the other hand, the negative ions stay in the electrolyte the entire time. The lithium ions (L_i^+) carry all of the charges via the electrolyte and across the separator diaphragm. Typically, the concentration of lithium $Li(s)$ on the electrode surface, the concentration of lithium-ion in the nearby electrolyte (L_i^+), and the potential drop between the electrode and electrolyte affect how quickly a reaction occurs on an electrode particle surface [1].

$$Li_s \rightleftharpoons Li^+ + e^-$$

In most cases, half-cell arrangements of the cells are tested before the assembly of full-cell. Half-cell is represented in conventional dimensions rather than in precise geometry and consists of a single electrode (testing material) and a reference electrode.

B. Mathematical Modelling of half-cell cathode

Drift-diffusion model has been applied to cell design by incorporating the practical dynamic electrochemical operations of Lithium ion batteries (see (1) – (5)) [13], [14]. For half-cell cathode, the anode is set as a reference electrode that is made entirely of lithium and a cathode is a working electrode. The anode serves as reference electrodes such that their electrochemical potential remains constant during charging and discharging. Hence, the anode potential is assumed to be zero while the potential at the cathode current collector determines the voltage drop across the half cell. Note that in this research, the model employs a linear diffusion equation to simulate the diffusion of Lithium in the electrode particles since diffusion in the nanoparticles does not significantly impact the results of discharge curves. Thus, an extremely fast diffusion model of electrode particles (see (6) – (7)) as suggested by Richardson et al. [15] is used. The battery model for half-cell cathode is given by [1] – [16];

$$\varepsilon_v \frac{\partial c}{\partial t} = \frac{\partial}{\partial x^*}\left(D(c)\beta \frac{\partial c}{\partial x^*}\right) - \frac{\partial t_+^0}{\partial x^*}\frac{\partial j}{F} + (1 - t_+^0) b_{et} G \,, \quad (1)$$

$$\frac{\partial j}{\partial x^*} = F B_{et} G \,, \quad (2)$$

$$j = -\beta \kappa(c)\left(\frac{\partial \phi}{\partial x^*} - \frac{2RT}{F}(1 - t_+^0)\frac{\partial \log c}{\partial x^*}\right) \,, \quad (3)$$

$$\eta = \phi - \phi_s - U_{eq}\left(c_s|_{r=a_0}\right) , \quad (4)$$

$$G = k_0(c)^{\frac{1}{2}}(c_s)^{\frac{1}{2}}\left(c_{s,max} - c_s|_{r=a_0}\right)^{\frac{1}{2}}\left(e^{\left(-\frac{F\eta}{2RT}\right)} - e^{\left(\frac{F\eta}{2RT}\right)}\right), \quad (5)$$

$$\frac{\partial c_s}{\partial t} = \frac{1}{r^2}\frac{\partial}{\partial r}\left(r^2 D_s(c_s)\frac{\partial c_s}{\partial r}\right), \quad (6)$$

$$\frac{\partial j_s}{\partial x^*} = FB_{et}G, \quad j_s = -\sigma_s\frac{\partial \phi_s}{\partial x^*} \quad , \quad (7)$$

with boundary conditions

$$c|_{x^*=0} = c_0, \quad D(c)\frac{\partial c}{\partial x^*}\Big|_{x^*=L} = 0 \quad (8)$$

,

$$\phi|_{x^*=0} = 0, \quad j|_{x^*=L} = 0 , \quad (9)$$

$$j_s|_{x^*=0} = 0 \quad j_s|_{x^*=L} = -\frac{I}{A}, \quad (10)$$

$$\frac{\partial c_s}{\partial r}\Big|_{r=0} = 0, \quad D_s(c_s)\frac{\partial c_s}{\partial r}\Big|_{r=a_0} = -G. \quad (11)$$

The parameters from Equation (1) to (11) are described in Table I. Equations (1) – (3) describe the charge carriers travel via a combination of diffusion and advection in an electric field which causes potential differences. The flux of lithium ions out of the cathode electrode particles (deintercalation/intercalation of ions) is determined by surface reaction rates (G). The intercalated lithium concentration on the electrode surface $\left(c_s|_{r=a_0}\right)$ and the ion concentration in the electrolyte (c) at the surface is determined by the Butler-Volmer equation (see (5)), which is phenomenological, and is typically used to model them. The surface reaction halts when the electrolyte concentration depletes $(c = 0)$ or when the lithium concentration on the electrode surface reaches maximum concentration $\left(c_s|_{r=a_0} = c_{s,max}\right)$. Here, it is assumed that every particle is electrically connected to the current collector and the potential of the negative electrode (anode) particles is zero to maintain universality [1]. The equilibrium potential, $U_{eq}(c_s)$ profiles vary with the intercalated lithium concentrations (c_s) on the electrode particles surface and are different for different cathode materials.

III. Numerical Procedure

The method of Lines (MOL) technique is a technique that converts the partial differential equations (PDEs) into a set of ordinary differential equations (ODEs) in time derivative by discretizing the spatial derivatives in (1) – (7) using centered difference approximation of finite difference method. The built-in solver '*ode15s*' in Matlab was used to solve the resulting ODEs forward in time.

The numerical scheme was developed based on the assumption that at each grid point of x (across the thickness of the electrode) there is a spherical particle (where radial diffusion of intercalated Li_s in the spherical particle occurs) and the particles touch each other. For example, for i grid points of x, the number of particles is i and each respective spherical particle is discretized radially by j grid points of r. If we take $i = 100$ grid points of x and $j = 100$ grid points of r for each spherical particle, the size of the numerical scheme is 10300×10300 entries of the differentiation matrix. The resulting differentiation matrix was a large system containing many zero elements; therefore, a Jacobian matrix was applied to improve the efficiency of the solver [3]. The parameter values used in the model are listed in Table II.

TABLE I
DESCRIPTION OF PARAMETERS

Electrolyte			
ε_v	Volume fraction	κ	Electrical conductivity
c	Lithium ion, Li^+ concentration	ϕ	Electrolyte potential
κ	Electrical conductivity	j	Current density
D	Diffusion coefficient	t_+^0	Transference number
Electrode particles			
c_s	Lithium, Li_s concentration	ϕ_s	Solid potential of cell
j_s	Current density	σ_s	Ionic conductivity
r	Distance from the center of electrode particle	a_0	Radius of electrode particle
Other parameters			
x	Distance of electrode	U_{eq}	Equilibrium cell potential
b_{et}	BET surface area	t	Time
F	Faraday constant	G	Reaction rate
R	Universal gas constant	η	Cell over-potential
β	Permeability tensor	L	Thickness of electrode

TABLE II
PARAMETER VALUES

Parameters	Value
Electrolyte Parameter $LiPF_6$ [4],[5]	
Diffusivity of $Li^+, D_0(m^2s^{-1})$	5.25×10^{-10}
Volume Fraction ϵ_v	0.4764
Initial Concentration $c_0(molm^{-3})$	1000
Transference Number t_+	0.38
Ionic Conductivity $\kappa_0(AVm^{-1})$	10^{-4}
Electrode Parameters for $LiFePO_4$ [1],[17],[18]	
Radius of Particle $a_0(m)$	5.2×10^{-8}
Diffusion coefficient $D_s(m^2s^{-1})$	6×10^{-18}
Exchange Current Density $k_0(Am^{-2})$	5.4×10^{-5}
Conductivity $\sigma_s(Sm^{-1})$	100
Electrode Thickness $L\ (m)$	6.2×10^{-5}
Max. Concentration $c_{s,max}(molm^{-3})$	18805
Electrode Parameters for $LiCoO_2$ [19],[20],[21]	
Radius of Particle $a_0(m)$	8.5×10^{-6}
Diffusion coefficient $D_s(m^2s^{-1})$	1×10^{-14}
Exchange Current Density $k_0(Am^{-2})$	5.4×10^{-5}
Conductivity $\sigma_s(Sm^{-1})$	10
Electrode Thickness $L\ (m)$	7.10×10^{-6}
Max. Concentration $c_{s,max}(molm^{-3})$	51555
Other Parameters [1]	
Faraday Constant $F\ (Cmol^{-1})$	96487
Gas Constant $R\ (Jmol^{-1}K^{-1})$	8.3144
BET surface area $bet\ (m^{-1})$	$\pi/2a_0$
Temperature $T\ (K)$	298
Permeability tensor β	$\epsilon_v^{1.5}$
Electrode Area $A\ (m^2)$	10^{-4}

IV. Results and Analysis

A. Experimental – simulation comparison

Fig. 2 and Fig. 3 were plotted at specific discharge rates; $0.8C$ for $LiFePO_4$ and $1C$ for $LiCoO_2$ (refer Table III and IV for the rate of current discharge in $mAhg^{-1}$). The solid line graphs represent the result from the numerical solution while the symbols graph represents the result from the experimental data. The figures showed that the discharge characteristics between these two materials are slightly different where the graph of the $LiFePO_4$ (refer Fig. 2) has a flat discharge curve until the cell is entirely discharged and $LiCoO_2$ (refer Fig.3) varies with changes in y (note that y is the amount of lithium inserted). The results from the model simulation show a good comparison with experimental data given by S. Erol [19] for $LiCoO_2$ and Owen et al. [18] for $LiFePO_4$.

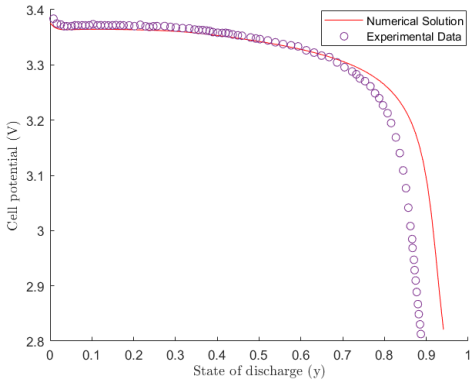

Fig. 2 The comparison between numerical solution and experimental data [18] of $LiFePO_4$ at 0.8C

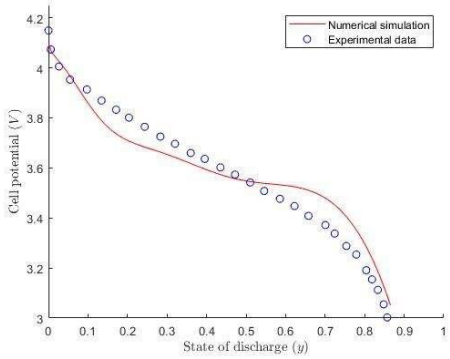

Fig. 3 The comparison between numerical solution and experimental data [19] of $LiCoO_2$ at $1C$

B. The Effect of Electrolyte Depletion on Different Discharge Currents

The electrolyte is a crucial component in Lithium ion battery as it facilitates the movement of ions between the positive and negative electrodes during the charging and discharging cycles. The concentration of lithium-ion decreases as the discharge current increases due to electrolyte depletion. As the discharge current increases, there can be limitations in the ability of the electrolyte to deintercalate/intercalate Lithium ions. Higher discharge currents can lead to reduced lithium-ion mobility within the cell, affecting the overall concentration of lithium ions available for discharge. The increase in discharge current can lead to higher internal resistance within the battery. This resistance, known as the Ohmic drop, results in voltage losses across the cell. The higher the internal resistance, the greater the voltage drop, which slightly affects the discharge characteristics as shown in Fig.17 at the beginning of discharge. The actual discharge currents in $mAhg^{-1}$sre given in Table III and IV.

The faster the discharge rate, the more demand there is for lithium ions to move between the anode and cathode. This increased demand can lead to localized depletion of lithium ions in the electrolyte near the electrode surfaces, contributing to a decrease in the overall concentration of lithium ions available for discharge. The results are shown in Fig. 4 until Fig. 6 for $LiFePO_4$ and Fig. 7 until Fig. 9 for $LiCoO_2$ for different discharge rates. Note that, the x-axis $\left(\frac{x^*}{L}\right)$ represents the dimensionless thickness of the cathode.

The graphs show that electrolyte concentration depletes as the lithium-ion travels from the electrolyte to the electrode surface particle to form a lithium solid. As the discharge rate increased, the speed of the lithium-ion travel via electrolyte increased where the rapid discharge occurs. At a higher discharge rate, the depletion of the lithium-ion $(c = 0)$ in the electrolyte increased. The active material in the solid cannot be discharged in the region of electrolyte depletion. Additionally, the conductivity of the electrolyte decreases as the electrolyte concentration approaches zero, significantly impeding discharge [1].

It can be proved by comparing Fig. 4 with Fig. 6, at 0.8C discharge rate referring to the green solid line, the electrolyte was in the depleted condition starting at about 92% state of discharge while for the 4C discharge rate, the depletion occurred at 19% state of discharge. The discharge rate is the factor that causes electrolyte depletion to increase.

For $LiCoO_2$ cell, the rate of electrolyte depletion shows the same area of electrolyte depletion as the discharge rate increased from 1C to 4C (see Fig.7 to Fig.9). It can be seen that the cell could have room for further discharge, however, it is hampered due to the solid state limitation as discussed in the next section.

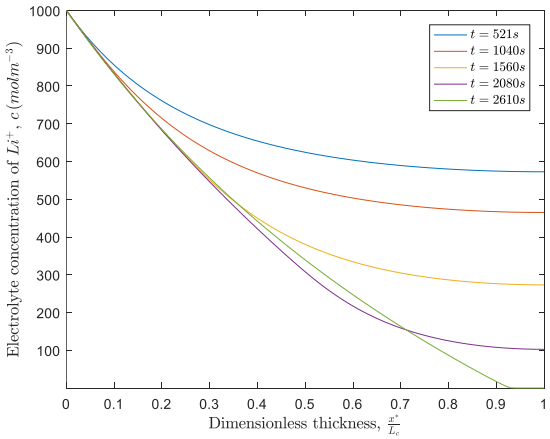

Fig. 4 The Lithium ion concentrations (c) in electrolyte measured at 0.8C for $LiFePO_4$.

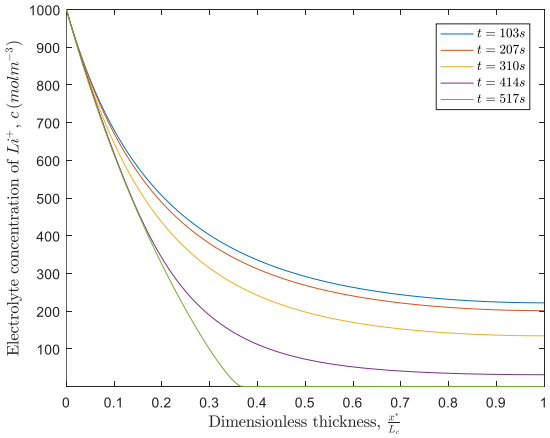

Fig. 5 The Lithium ion concentrations (c) in electrolyte measured at 2C for $LiFePO_4$.

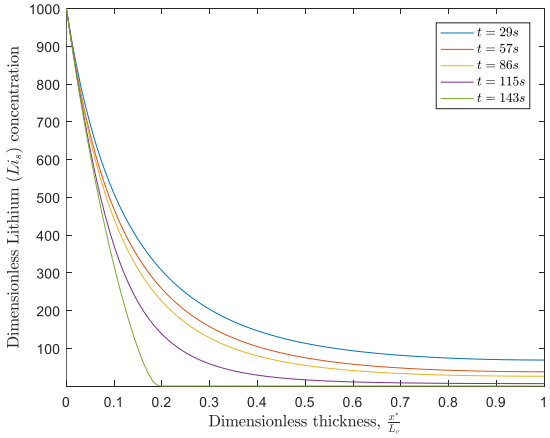

Fig. 6 The Lithium ion concentrations (c) in electrolyte measured at 4C for $LiFePO_4$.

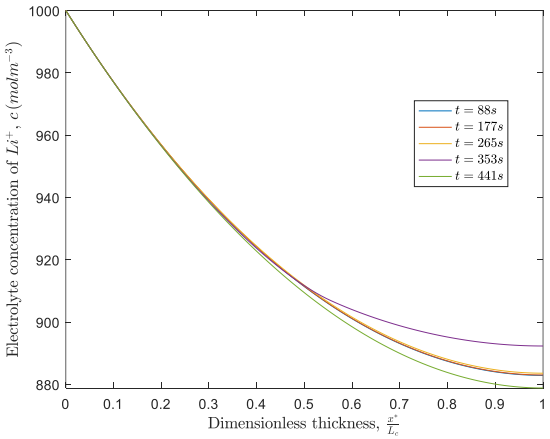

Fig. 7 The Lithium ion concentrations (c) in electrolyte measured at 1C for $LiCoO_2$.

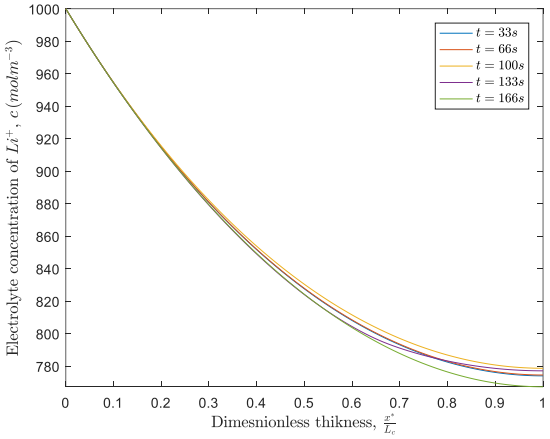

Fig. 8 The Lithium ion concentrations (c) in electrolyte measured at 2C for $LiCoO_2$.

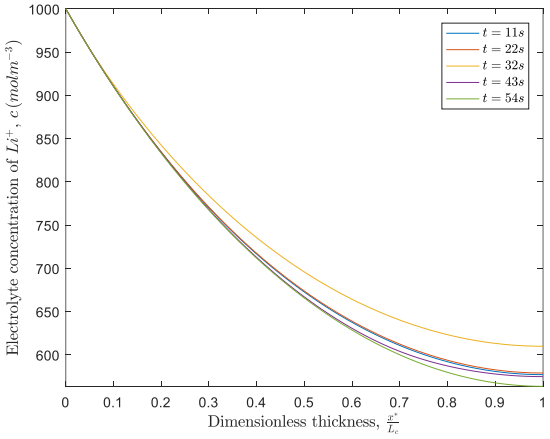

Fig. 9 The Lithium ion concentrations (c) in electrolyte measured at 4C for $LiCoO_2$.

C. The Effect of Electrode Particles Limitation on Different Discharge Currents

The maximum lithium concentration in a lithium-ion battery is mainly determined by the properties of the electrode materials. The concentration of lithium ions in the electrolyte also plays a role. Different cathode materials have different lithium storage capacities. The maximum lithium concentration is influenced by the specific chemical structure and capacity of the cathode material. It can be seen in Table II where the maximum lithium concentration of $LiCoO_2$ is 51410 molm^{-3} which is much higher than $LiFePO_4$, 18805 molm^{-3}. The discussion is to clarify how the discharge rate affects the concentration of electrolytes and the discharge of electrode particles. Here we address that there are differences of the radius of particles for $LiFePO_4$ and $LiCoO_2$ which are nano-sized ($5.2 \times 10^{-8} m$) and micro-sized ($8.5 \times 10^{-6} m$), respectively.

The intercalation takes place when a lithium-ion intercalates with an electron to form a lithium solid which then diffuses in the electrode particle. The solid concentration is shown in Fig. 10 to Fig. 12 for $LiFePO_4$ and Fig. 13 to Fig. 15 for $LiCoO_2$.

Note that, based on the figures plotted, the y-axis ($c_s|_{r=1}$) represents the dimensionless concentration of Lithium solid (the actual concentration divided by the maximum concentration) at the particle surface. $c_s|_{r=1} < 0$ indicates that there is a vacancy in the electrode particles for intercalation while $c_s|_{r=1} = 1$ shows that the electrode particles have reached maximum concentration and are fully discharged. Thus, the intercalation hampers because of no vacancy in the electrode particles to intercalate. The shaded regions represent the region of electrolyte depletion.

The nano-sized electrode particles of $LiFePO_4$ ensure a rapid diffusion in particles. It is seen in Fig. 10 to Fig. 12 that shows the particles near the separator are fully discharged. Two regions appear, one with the electrode particles fully discharged and the other with vacancy. However, due to the increase of electrolyte depletion region (see Fig. 4 to Fig.6) the discharge cannot go further since there is no lithium ion to cause the surface reaction. Hence, the cell performances deteriorate as discharge currents increase as shown in Fig.17. At discharge rate of 0.8C (refer to Fig. 10), the electrolyte depletion region is small indicating that at a low discharge rate, loads of lithium can be intercalated meanwhile at higher discharge rates (refer to Fig. 11 – Fig. 12), the electrolyte depletion region is getting bigger causing the decrease in lithium ion to intercalate due to the active material in the solid cannot be discharged in the areas where the electrolyte has become depleted.

In $LiCoO_2$, it can be seen that different phenomenon occurs (refer to Fig. 13 to Fig. 15). The particles discharge almost uniformly across the thickness of the cell. Simultaneous with the same pattern of electrolyte depletion of $LiCoO_2$, the intercalation of Lithium at the particle surface occurs rapidly and becomes saturated with Lithium, hence limiting the discharge. However, the lithium ion is being discharged layer by layer or from bottom to top, which is different from the $LiFePO_4$, where the lithium-ion that is nearest to the separator is discharging until it is fully discharged. This can be explained by the size of particles which is macro-sized, 10^2 larger than $LiFePO_4$. Following this, the discharge of $LiCoO_2$ is thus limited by the fast Lithium intercalation on the electrode particle surface.

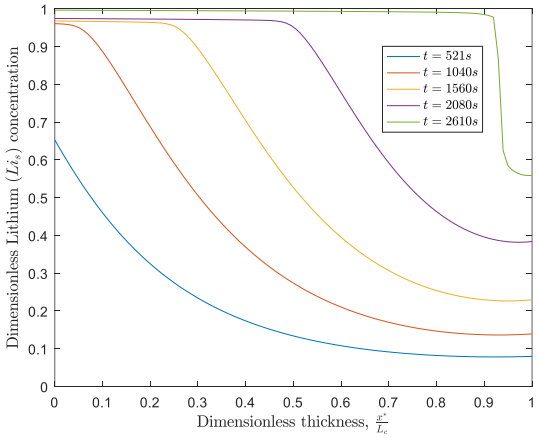

Fig. 10 Dimensionless Lithium Concentration on the electrode particle surface $\left(\frac{c_s|_{r=a_0}}{c_{s,\max}}\right)$ measured at 0.8C for $LiFePO_4$.

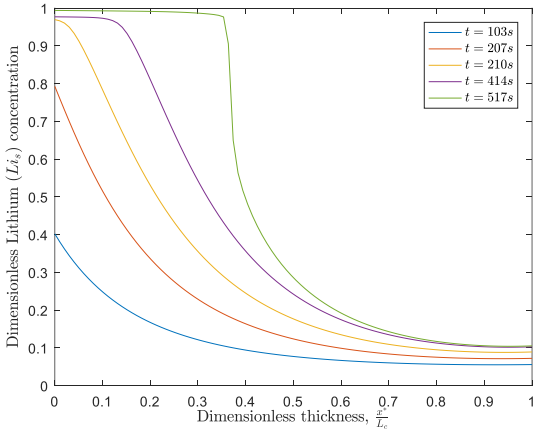

Fig. 11 Dimensionless Lithium Concentration on the electrode particle surface $\left(\frac{c_s|_{r=a_0}}{c_{s,\max}}\right)$ measured at 2C for $LiFePO_4$.

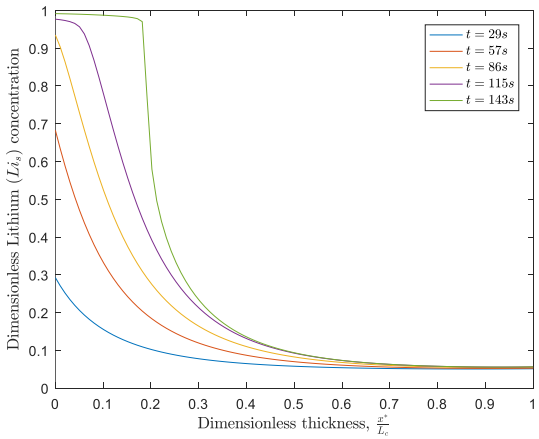

Fig. 12 Dimensionless Lithium Concentration on the electrode particle surface $\left(\frac{c_s|_{r=a_0}}{c_{s,\max}}\right)$ measured at 4C for $LiFePO_4$.

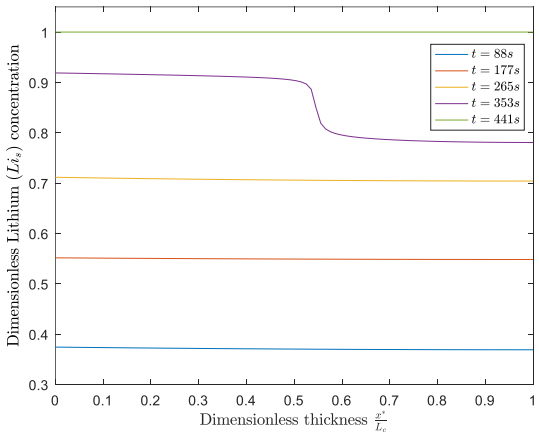

Fig. 13 Dimensionless Lithium Concentration on the electrode particle surface $\left(\frac{c_s|_{r=a_0}}{c_{s,\max}}\right)$ measured at 1C for $LiCoO_2$.

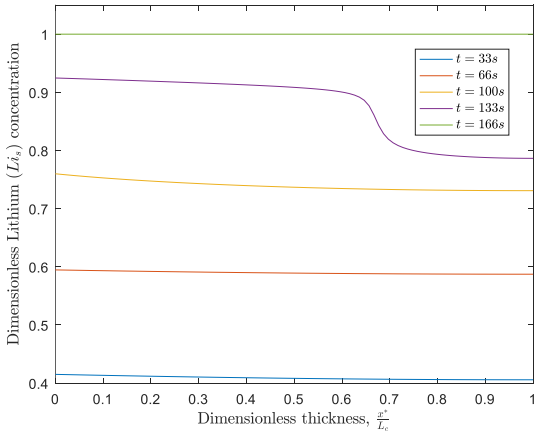

Fig. 14 Dimensionless Lithium Concentration on the electrode particle surface $\left(\frac{c_s|_{r=a_0}}{c_{s,\max}}\right)$ measured at 2C for $LiCoO_2$.

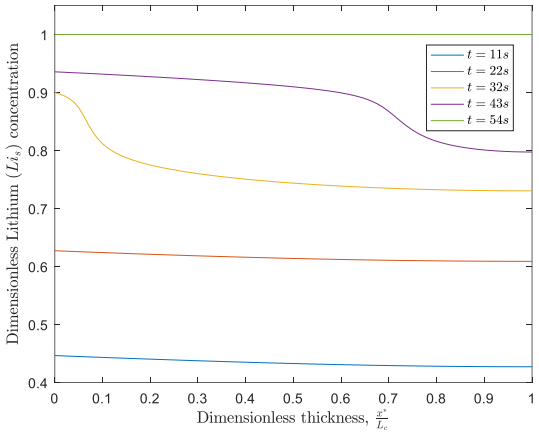

Fig. 15 Dimensionless Lithium Concentration on the electrode particle surface $\left(\frac{c_s|_{r=a_0}}{c_{s,\max}}\right)$ measured at 4C for $LiCoO_2$.

V. The Cell Performance of $LiFePO_4$ and $LiCoO_2$ cell on Different Discharge Currents

Each cathode material has a different maximum concentration and the discharge process is observed based on different discharge rates as listed in Table III and Table IV.

Fig. 16 and Fig. 17 demonstrate the discharge curves for different discharge rates for $LiFePO_4$ and $LiCoO_2$, respectively. The curve becomes steeper to represent the battery discharging rapidly at a higher discharge rate.

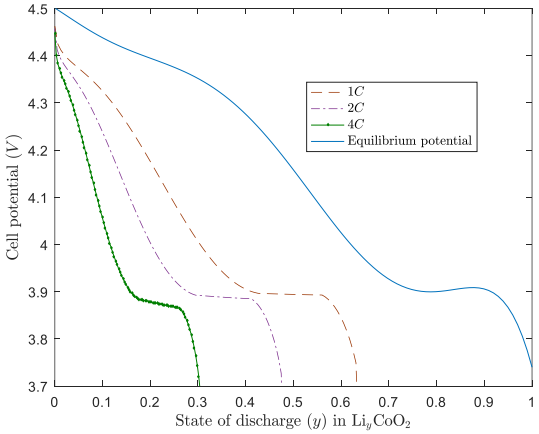

Fig. 16 Discharge Curves of $LiCoO_2$ at different discharge currents

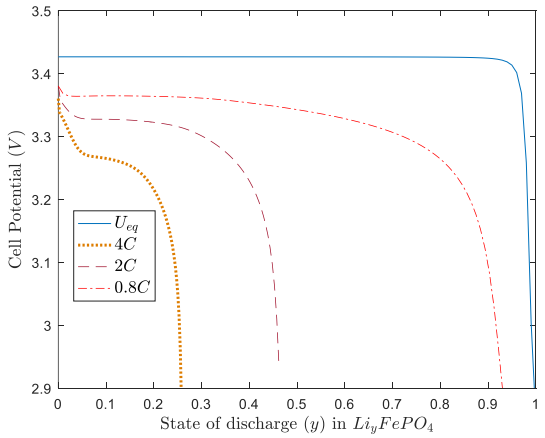

Fig. 17 Discharge Curves of $LiFePO_4$ at different discharge currents

TABLE III
DISCHARGE CONCENTRATION AND DISCHARGE CURRENT FOR 1C, 2C, 4C $LiCoO_2$

$LiCoO_2$

C-Rate	Percentage Performance (%)	Max. Concentration ($molm^{-3}$)	Discharge Concentration ($molm^{-3}$)	Discharge Current ($mAhg^{-1}$)
1C	97.16%		49949.96	279.49
2C	49.79%	51555	25597.04	286.45
3C	30.03%		15438.42	259.15

TABLE IV
ACTUAL CONCENTRATION AND DISCHARGE CURRENT FOR 0.8C, 2C, 4C $LiFePO_4$

$LiFePO_4$

C-Rate	Percentage Performance (%)	Max. Concentration ($molm^{-3}$)	Actual Concentration ($molm^{-3}$)	Discharge Current ($mAhg^{-1}$)
0.8C	96.45%		18137.42	108.03
2C	48.65%	18805	9148.63	136.22
4C	28.76%		5408.32	161.06

The increase in discharge rate causes the percentage concentration over maximum concentration to start to drop as shown in Table III and Table IV. At low discharge 0.8C for $LiFePO_4$ and 1C for $LiCoO_2$, the percentage of concentration is above 90%, meaning the cells operate at high capacity while at higher discharge, 3C for $LiFePO_4$ and 4C for $LiCoO_2$, the percentage of concentration is below 30% due to the large electrolyte depletion region (see Fig. 6 and Fig. 9). Furthermore, the time frame for a $LiCoO_2$ cell to stop discharging is shorter than $LiFePO_4$ regardless it has higher maximum Lithium concentration that can facilitate the discharge. It can be seen in the comparison of the end time of discharge at 2C discharge rate in Fig.11 for $LiFePO_4$ which took 517 seconds and Fig.14 for $LiCoO_2$, 166 seconds.

During low discharge rate, the electrolyte depleted near to separator, making the electrode particle that far from the separator accessible and continue to discharge. However, for higher discharge rate it is vice versa where the concentration of the electrolyte is depleted near the current collector, so the electrode particle which is far from the separator cannot be accessible for the lithium ion to intercalate with an electron at the electrode particles surface.

By comparing the value of discharge current for both materials at the same discharge rate at 2C (refer Table III and Table IV), the value discharge current for $LiCoO_2$ is greater than the $LiFePO_4$. This is because $LiCoO_2$ has a higher maximum concentration than $LiFePO_4$. The higher the maximum concentration, the more intercalation process can occur. Despite such an advantage, the $LiCoO_2$ voltage drops gradually with changes in the amount of lithium inserted as the battery is discharging. This might result in capacity decay. Meanwhile, $LiFePO_4$ has the characteristic of a flat discharge curve which gives almost the same power with changes of the inserted lithium until the cell is entirely discharged.

VI. Conclusion

In conclusion, the half-cell cathode of Lithium ion battery is discussed. Numerical solutions using Method of Lines techniques are simulated to generate the solution to the mathematical model of the half-cell cathode. Two types of cathode material, namely $LiFePO_4$ and $LiCoO_2$ which have different discharge characteristics were studied and their performances were analyzed. When the discharge rate increases, the drop in discharge capacity occurs due to the large region of electrolyte depletion. The primary cause of the abrupt reduction in cell potential at low electrode utilization is the slow rate of transport in the electrolyte phase. As the discharge rate increases, the electrolyte concentration drops to zero as Lithium ion approaches the current collector, making it hard to access electrode particles far from the separator hence hampering the discharge. It is believed that the results may be useful for selecting suitable cathode material for different applications.

Acknowledgement

The authors would like to thank the Universiti Teknikal Malaysia Melaka for the research support.

Conflict of Interest

The authors declare no conflict of interest in the publication process of the research article.

Author Contributions

Author 1: Simulation data, analysis, writing, draft preparation; Author 2: Supervision, coding development, draft review and editing; Author 3: Numerical procedure; Author 4: Review.

References

[1] Rahifa Ranom, "Mathematical modeling of lithium-ion battery," in Ph.D. thesis., Fac. Of Soc and Human Sci., University of Southampton., UK. 2014. Accessed on: June 26, 2021. [Online]. Available

[2] S. Liu, J. Chen, C. Zhang, L. Jin, and Q. Yang, "Experimental study on lithium-ion cell characteristics at different discharge rates," *J. Energy Storage*, vol. 45, Jan. 2022, doi: 10.1016/j.est.2021.103418.

[3] Yuanyuan, Liu., Hao, Liu., Liwei, An., Xinxin, Zhao., Guangchuan, Liang. Blended spherical lithium iron phosphate cathodes for high energy density lithium–ion batteries. *Ionics*, 2019, doi: 10.1007/S11581-018-2566-7

[4] Yuanyuan, Liu., Hao, Liu., Liwei, An., Xinxin, Zhao., Guangchuan, Liang. Blended spherical lithium iron phosphate cathodes for high energy density lithium–ion batteries. *Ionics*, 2019 doi: 10.1007/S11581-018-2566-7

[5] Zeqing, Duan., Yunfan, Wu., Jie, Lin., Laisen, Wang., Dong-Liang, Peng. Thin-Film Lithium Cobalt Oxide for Lithium-Ion Batteries. *Energies*, 2022, doi: 10.3390/en15238980

[6] D. Inayat, Ali, Khan., Fatima, Nasim., Mohammad, Choucair., Sana, Ullah., Amir, Badshah., Muhammad, Nadeem. Cobalt oxide nanoparticle embedded N-CNTs: lithium ion battery applications. *RSC Advances*, 2016 doi: 0.1039/C5RA23222H

[7] Ankit, Verma., David, R., Corbin., Mark, B., Shiflett. Lithium and cobalt recovery for lithium-ion battery recycle using an improved oxalate process with hydrogen peroxide. *Hydrometallurgy*, 2021 doi: 10.1016/J.HYDROMET.2021.105694

[8] Florian, Hall., Sabine, Wußler., Hilmi, Buqa., Wolfgang, G., Bessler. (2016). Asymmetry of Discharge/Charge Curves of Lithium-Ion Battery Intercalation Electrodes. *Journal of Physical Chemistry*, doi: 10.1021/ACS.JPCC.6B07949

[9] Qi, Liu., Xin, Su., Dan, Lei., Yan, Qin., Jianguo, Wen., Fangmin, Guo., Yimin, A., Wu., Yangchun, Rong., Ronghui, Kou., Xianghui, Xiao., Frederic, Aguesse., Javier, Bareño., Yang, Ren., Wenquan, Lu., Yangxing, Li. Approaching the capacity limit of lithium cobalt oxide in lithium-ion batteries via lanthanum and aluminium doping, *Nature Energy*, 2018.

[10] R. Sharma, Rahul, M. Sharma, and J. K. Goswamy, "Li-ion battery: Lithium cobalt oxide as cathode material," in *AIP Conference Proceedings, American Institute of Physics Inc*., Nov. 2020. doi: 10.1063/5.0017341.

[11] Junsheng, Zhu., Xiaobo, Ding. (2019). Embedding cobalt sulfide in reduced graphene oxide for superior lithium-ion storage. *Materials Letters*, doi: 10.1016/J.MATLET.2019.06.020

[12] Luis. D. Couto, M. Charkhgard, B. Karaman, N. Job, and M. Kinnaert, "Lithium-ion battery design optimization based on a dimensionless reduced-order electrochemical model," *Energy*, p. 125966, Jan. 2022, doi: 10.1016/j.energy.2022.125966.

[13] V. Srinivasan and J. Newman, "Discharge Model for the Lithium Iron-Phosphate Electrode," *J Electrochem Soc*, vol. 151, no. 10, p. A1517, 2004, doi: 10.1149/1.1785012.

[14] T. F. Fuller, M. Doyle, and J. Newman, "Electrochemical Science And Technology Simulation and Optimization of the Dual Lithium Ion Insertion Cell," *J Electrochem Soc*, vol. 141, no. 1, 1994, doi:10.1149/1.2054684

[15] G.W. Richardson, J.M. Foster, R. Ranom, CP Please, AM Ramos, Charge transport modelling of Lithium-ion batteries; *European Journal of Applied Mathematics* 33 (6), 983-1031,2020

[16] Ranom R., Rosszainily H.N.A., Lithium ion battery performance for different size of electrode particles and porosity, *International Journal of Innovative Technology and Exploring Engineering*, 9 (1), pp. 4401 – 4405, 2019, DOI: 10.35940/ijitee.A5086.119119

[17] Ranom R., Bacho R.S., Jamal S.N.A.S.A., The effect of electrolyte parameter variation upon the performance of lithium iron phosphate (LiFePO4), *Indonesian Journal of Electrical Engineering and Computer Science*, 28 (1), pp. 58 – 66, 2022, DOI: 10.11591/ijeecs.v28.i1.pp58-66

[18] Johns P.A., Roberts M.R., Wakizaka Y., Sanders J.H. and Owen J.R., How the electrolyte limits fast discharge in nanostructured batteries and supercapacitors, *Electrochem. Comm.* 11, 2089-2092, 2010.

[19] S. Erol, "Electrochemical Impedance Spectroscopy Analysis And Modeling Of Lithium Cobalt Oxide/Carbon Batteries," 2015.

[20] F. Jiang and P. Peng, "Elucidating the Performance Limitations of Lithium-ion Batteries due to Species and Charge Transport through Five Characteristic Parameters," Sci Rep, vol. 6, Sep. 2016, doi: 10.1038/srep32639.

[21] D. M. Rosewater, D. A. Copp, T. A. Nguyen, R. H. Byrne, and S. Santoso, "Battery Energy Storage Models for Optimal Control," IEEE Access, vol. 7, pp. 178357–178391, 2019, doi: 10.1109/ACCESS.2019.2957698.